Detection of Atherosclerotic Plaques in the Rabbit Aorta Using Ultrasound Microbubbles Conjugated to Interleukin-18 Antibodies

Authors' Contribution:
Study Design A
Data Collection B
Statistical Analysis C
Data Interpretation D
Manuscript Preparation E
Literature Search F
Funds Collection G

ABE 1 Zhen-zhen Jiang
BD 1 Xia-tian Liu
BC 1 Cai-ye Ma
BF 2 Cong He
BD 1 Xing-yun Li
BD 3 Chuan-lin Hou
BC 4 Zu-sheng Cheng
ADG 1 Guo-yuan Xia

1 Department of Ultrasound, Shaoxing People's Hospital (Shaoxing Hospital of Zhejiang University), Shaoxing, Zhejiang, P.R. China
2 Department of Radiology, Shaoxing Second Hospital, Shaoxing, Zhejiang, P.R. China
3 Department of Pathology, Shaoxing People`s Hospital (Shaoxing Hospital of Zhejiang University), Shaoxing, Zhejiang, P.R. China
4 Department of Radiology, Shaoxing Seventh Hospital, Shaoxing, Zhejiang, P.R. China

Corresponding Author: Guo-yuan Xia, e-mail: fjzzjzz02@sina.com
Source of support: This work was supported by the Zhejiang Medical Scientific Research Foundation (NO. 2015KYA220) and Shaoxing Nonprofit Technology Applied Research Projects (NO. 2014B70053)

Background: The purpose of the study was to investigate the ability of microbubbles (MBs) targeting interleukin-18 (IL-18) to detect plaques in a rabbit atherosclerotic plaque model.

Material/Methods: A rabbit atherosclerotic plaque model was established. The locations of the atherosclerotic plaques were verified by two-dimensional scanning and color Doppler flow imaging. An IL-18 antibody was conjugated to naked MBs (MB_c) using the biotin-streptavidin conjugation method, resulting in the formation of MB_{IL-18}. MB_c and MB_{IL-18} were then used for contrast-enhanced ultrasound (CEUS) studies. The locations of CD34 and IL-18 within the plaques were determined by immunohistochemistry, and IL-18 expression levels in the plaques were determined by Western blot analysis. The relationships between IL-18 expression and the contrast intensity of the 2 MBs were analyzed.

Results: MB_c and MB_{IL-18} were both uniformly dispersed. Fluorescence microscopy and flow cytometry revealed that IL-18 was successfully conjugated to MBs. CEUS images showed that the intensity of the MB_{IL-18} signal was substantially enhanced and prolonged compared with that of the MB_c signal. Immunohistochemistry showed that CD34 expression was significantly increased in the plaques and that IL-18 was mainly located in the inner parts and base of the atherosclerotic plaques. Western blot analysis revealed that IL-18 expression was higher in the plaque regions. Correlation analysis showed that IL-18 expression was correlated with the contrast intensity of MB_{IL-18} ($r=0.903$, $P<0.05$) but not with MB_c ($r=0.540$, $P>0.05$).

Conclusions: MBs targeting IL-18 may be a novel, noninvasive method of diagnosing atherosclerotic plaques.

MeSH Keywords: Microbubbles • Plaque, Atherosclerotic • Ultrasonography, Doppler

Full-text PDF: https://www.medscimonit.com/abstract/index/idArt/907572

📄 2404   ▦ 1   📊 6   📚 25

Background

Atherosclerosis is a systemic pathological process that affects large arteries throughout the body [1]. During atherosclerosis, plaques form on arterial walls, and the progression of such plaques can lead to arterial occlusion, which prevents organs from receiving oxygen, blood, and vital nutrients. Therefore, the identification of atherosclerotic plaques, especially vulnerable atherosclerotic plaques, is necessary to guide the management and prevention of severe cardiovascular events, such as stroke and myocardial infarction [2,3].

Previous studies have shown that contrast-enhanced ultrasound (CEUS) improves ultrasound images of atherosclerotic plaques by more accurately delineating the vascular wall and enhancing the visualization of the vascular lumen [4,5]. Additionally, CEUS can also show the adventitia that nourishes atherosclerotic vessels and demonstrate intraplaque neovascularization [6–8]. The development of new molecular imaging technologies has facilitated the performance of CEUS with targeted microbubbles (MBs) [9]. This imaging technique has shown promise as a noninvasive method for evaluating vulnerable atherosclerotic plaques. Previous studies of targeted MBs have mainly focused on vascular cell adhesion molecule-1 [10], junctional adhesion molecule-A [11], glycoprotein VI [12], glycoprotein IIb/IIIa [13], and other similar molecules. However, thus far, there have been no reports on the detection of atherosclerotic plaques by MBs targeting interleukin-18 (IL-18), which plays an important role in atherosclerotic plaque instability and rupture.

Hence, in the present study we prepared MBs targeting IL-18, evaluated the relationship between IL-18-targeted MB retention and IL-18 expression in a rabbit atherosclerotic plaque model, and investigated whether IL-18-targeting MBs are useful for identifying atherosclerotic plaques.

Material and Methods

Animal models

Twenty male Japanese white rabbits (2.0–2.5 kg, 2 months old) were housed and handled in accordance with the guidelines developed by the Institutional Animal Research Committee. Fourteen of these rabbits were subjected to the atherogenic protocol as previously described, with minor modifications [14]. Briefly, to induce atherosclerotic plaque formation, we fed the rabbits a high-fat diet (1% cholesterol and 8% lard) for 8 weeks, during which they were subjected to immune-mediated vascular intimal injury induced by intravenous injections of bovine serum albumin (25 mg/kg every 3 days for a total of 3 injections). The modeling process was monitored by ultrasonic examination.

The remaining 6 rabbits (age- and weight-matched) served as untreated, non-atherosclerotic control rabbits. Serum lipid levels, including total cholesterol (TC), triglyceride (TG), and low-density lipoprotein (LDL) levels, were determined at baseline and during the 8th week of the experiment.

MB preparation

We prepared a solution of streptavidin-coated MBs (Targestar-SA, Targeson, San Diego, CA, USA; distributed by Origin Biosciences in China) with a mean diameter of approximately 2.0 µm at a concentration of approximately 1×10^9 particles per milliliter. The MBs were then conjugated to biotinylated antibodies against IL-18 (BIOSS, Beijing, China) via biotin-streptavidin conjugation, as previously described [15]. Briefly, before conjugation, the vial containing the MBs was gently shaken end-to-end for 10 s to disperse them. Approximately 200 µg of biotinylated antibody was conjugated to 1.5×10^9/mL streptavidin-coated MBs, and then the resulting mixture was incubated for approximately 20 min at room temperature. Any unbound antibodies were subsequently removed by centrifugation and washing, yielding a solution of MBs that target IL-18 (MB_{IL-18}). Unconjugated Targestar-SA MBs (MB_c) were used as a negative control.

Characterization of the targeted MBs

The MB_{IL-18} and MB_c suspensions were each smeared onto glass slides, and their structural properties, sizes, shapes, and concentrations were studied under an optical light microscope. To measure conjugation efficiency, we incubated MB_{IL-18} with FITC-conjugated anti-rabbit IgG secondary antibodies for 30 min at room temperature. After the free secondary antibodies were removed, the targeted MBs were isolated for fluorescence microscopy and flow cytometry analyses.

CEUS imaging of atherosclerotic plaques

The rabbits were anesthetized with an intraperitoneal injection of 3% pentobarbital sodium (1 mL/kg) and placed in the supine position before undergoing ultrasound examination. An ultrasound imaging system (Philips IE33 Ultrasound, Philips Medical Systems, USA) and an L9-3 linear transducer transmitting at a frequency of 7 MHz were used to acquire CEUS images of the abdominal aorta. The imaging frame rate was set at 50 Hz, the mechanical index (MI) was set at 0.08, and the dynamic range was set at 50 dB. All parameters were kept constant during the examination.

A conventional two-dimensional ultrasound scan was first conducted to screen for clearly visible atherosclerotic plaques, and CEUS was initiated when such atherosclerotic plaques were observed. CEUS was performed first with MB_c and then with

Table 1. Blood biochemical examination between the two groups.

Group	Number	TC		TG		LDL-C	
		0 w	8 w	0 w	8 w	0 w	8 w
Control group	6	2.64±0.97	2.94±1.31	1.53±0.66	1.79±0.99	1.41±0.93	1.76±1.24
Model group	10	2.70±0.90	36.99±4.46*	1.30±0.52	2.84±2.55*	1.73±0.70	24.61±3.96*

Values are provided as mean ±SD (mmol/L). After 8 weeks, significant difference between the two groups (* $P<0.05$).
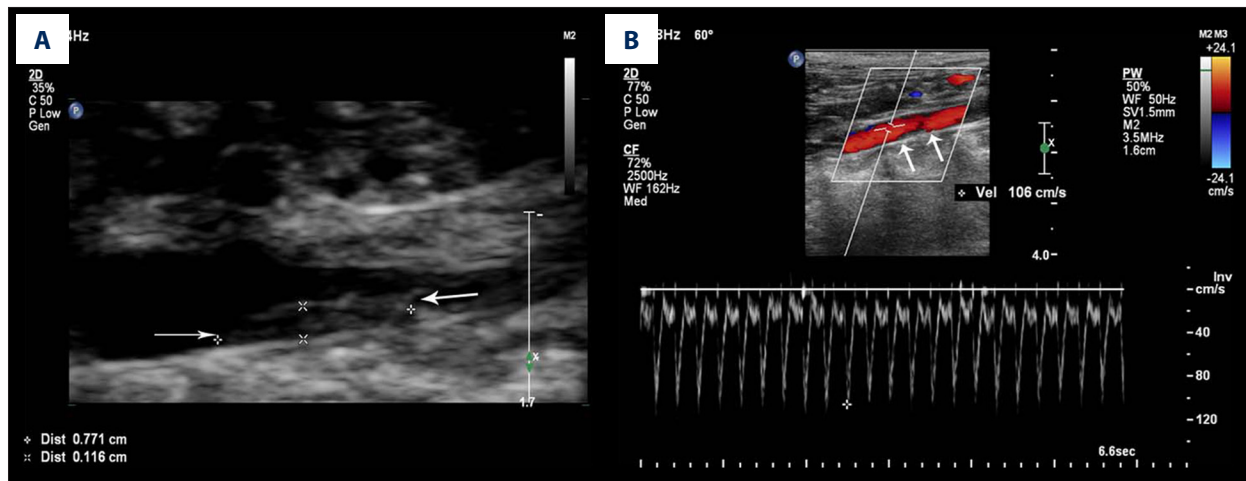

Figure 1. Representative ultrasound images of plaques in rabbits. (**A**) Two-dimensional imaging of a plaque in a rabbit aorta. The plaque is indicated by arrowheads. (**B**) Color Doppler flow imaging of the plaque. A filling defect was detected at the position of the atherosclerotic plaque, which is indicated by arrowheads.

MB_{IL-18} 30 min later (to allow clearance of the MBs injected previously). The MBs were administered at a dose of 0.05 mL/kg by bolus retro-orbital injection via the auricular vein, and then 1 mL of saline was infused to flush the duct. Immediately after MB injection, we initiated a contrast-enhanced program to acquire continuous dynamic images over a period of 90 s post-injection. All digital images were stored for offline examination.

CEUS image analysis

CEUS image quantification was performed to acquire the acoustic signals backscattered by the MBs. To assess the extent to which the 2 MBs enhanced the atherosclerotic plaques, we manually drew a region of interest (ROI) around the plaque and kept each ROI at almost the same size. The grayscale values within the ROI were quantified using the Image-Pro Plus Image Analysis System (Media Cybernetics, USA), and a time-intensity curve (TIC) was generated to compare the intensities of the signals from the 2 MBs in the atherosclerotic plaques.

Histopathology and immunohistochemistry

The aorta samples were fixed in 4% paraformaldehyde and then embedded in paraffin for histopathologic examination.

The paraffin-embedded sections were then subjected to hematoxylin and eosin staining and immunohistochemical analysis. Immunostaining was performed to determine the locations of CD34 and IL-18 proteins within the plaques. The sections were incubated with primary antibodies against CD34 (1: 400, Abcam, Cambridge, UK) and IL-18 (1: 400 dilution, Abcam, Cambridge, UK) overnight at 4°C before incubation with the appropriate secondary antibodies (1: 2000, ZSGB-BIO, Beijing, China) for 30 min at room temperature. Then, they were stained with diaminobenzidine and mounted with a neutral resin medium.

Western blot assay

IL-18 protein expression was assessed by Western blot analysis. The targeted proteins in the abdominal aorta samples were extracted by tissue homogenization, isolated by SDS-PAGE electrophoresis, and then transferred to nitrocellulose membranes, which were blocked with 5% non-fat dried milk before incubation with primary antibodies against IL-18 (1: 5000 dilution, Abcam, Cambridge, UK) overnight at 4°C. The proteins were then incubated with the appropriate horseradish peroxidase-conjugated IgG secondary antibodies (1: 5000, ZSGB-BIO, Beijing, China) for 1 h. The bands were detected using an ECL kit, and the signals were captured on X-ray film.
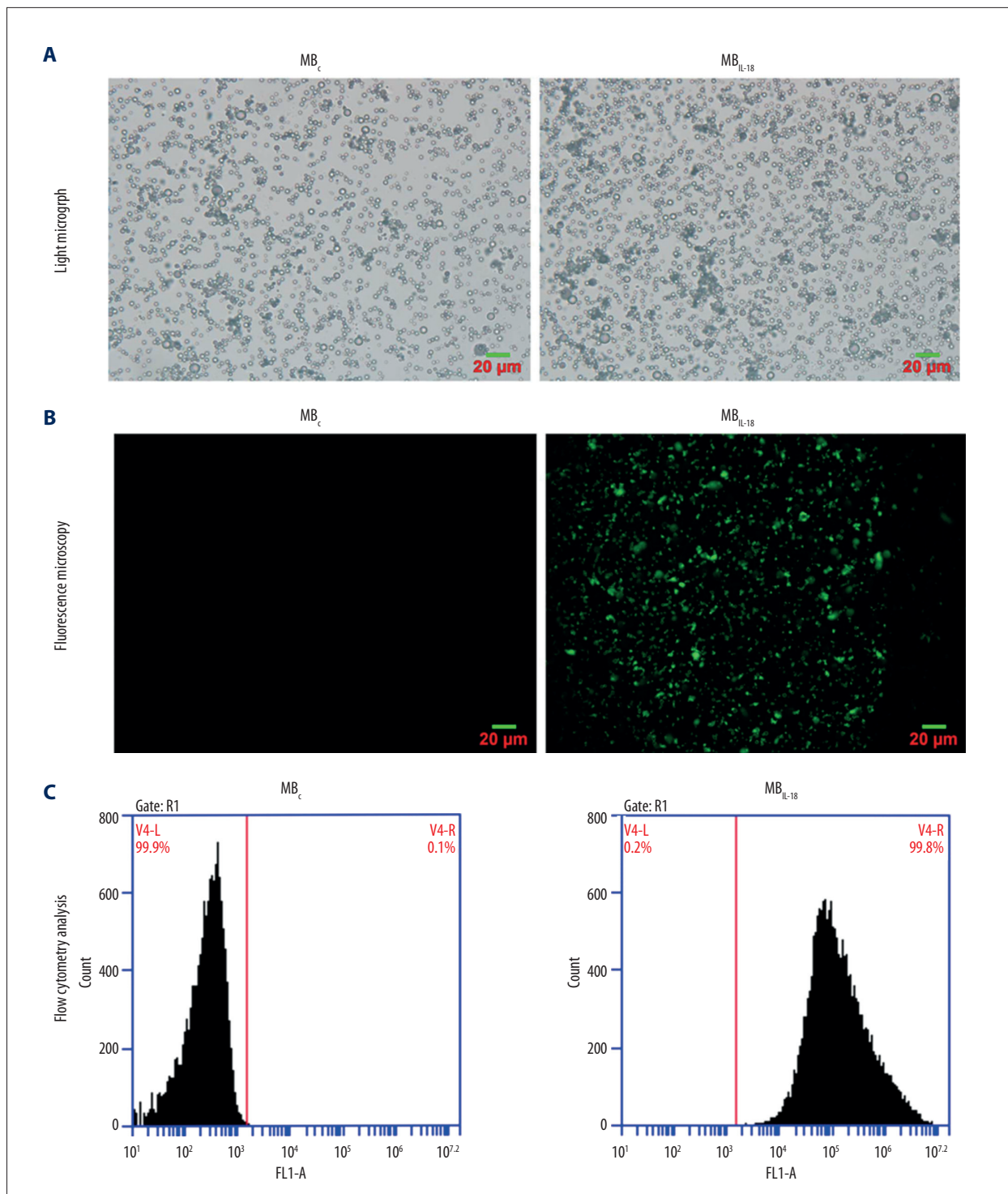
Figure 2. Characterization of MBs. (**A**) Light microscopy showed that the distribution of the 2 MBs was uniform with a single and scattered pattern. (**B**) Fluorescence microscopy revealed no fluorescence signal on the surface of MB$_c$, but there was a notable green fluorescence signal from the surface of MB$_{IL-18}$. (**C**) Flow cytometry revealed that the IL-18 antibody was successfully conjugated to the microbubbles.
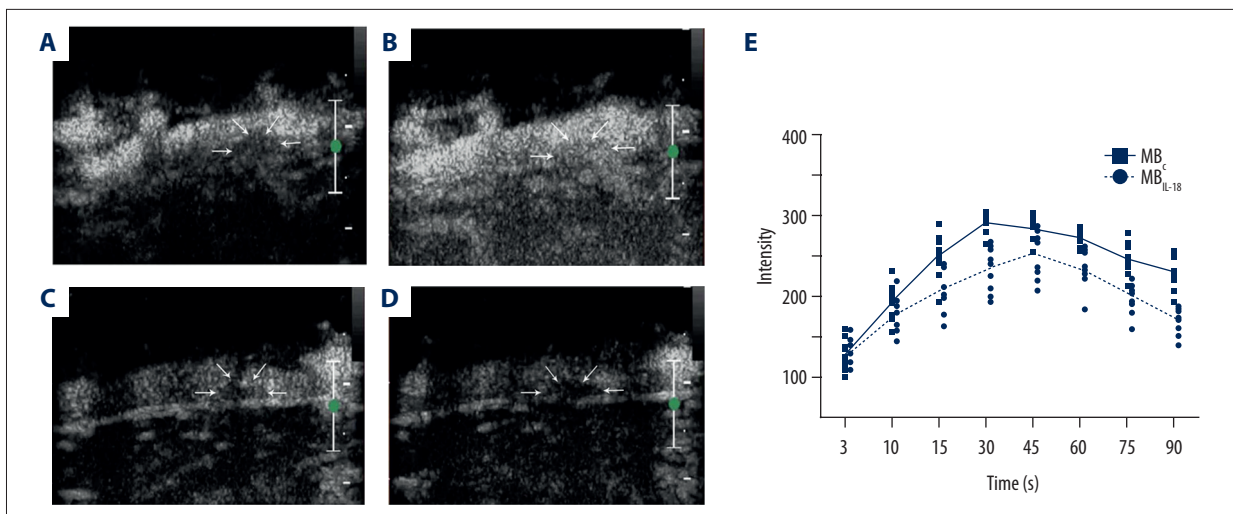
Figure 3. Sequential contrast-enhanced ultrasound images of atherosclerotic plaques in MB_{IL-18}-treated rabbits. (**A**) Ten seconds after the injection of MB_{IL-18}. The plaque is indicated by arrowheads. (**B**) Thirty seconds after the injection of MB_{IL-18}. The plaque is indicated by arrowheads. (**C**) Sixty seconds after the injection of MB_{IL-18}. The plaque is indicated by arrowheads. (**D**) Ninety seconds after the injection of MB_{IL-18}. The plaque is indicated by arrowheads. (**E**) The time-intensity curve based on MB_c and MB_{IL-18} showed that the peak times were earlier and peak intensities were higher in the MB_{IL-18} images than in the MB_c images, and the contrast duration was also longer.

Statistical analysis

The data were analyzed using SPSS 21.0 (SPSS Inc., Chicago, IL, USA). Quantitative results are presented as the mean ± standard deviation, and the significance of the differences between groups was determined with the Student's *t* test. Comparisons between the naked and targeted MBs were performed with paired *t* tests. Correlations between protein expression and CEUS results were assessed by Pearson correlation analysis. A *P* value less than 0.05 was considered statistically significant.

Results

Rabbit atherosclerotic plaque model

In this study, the survival rates in the control (n=6) and model groups (n=10) were 100% and 80%, respectively. Two of the rabbits in the model group died after being injected with bovine serum albumin: 1 died of malnutrition and 1 died of unknown causes. As expected, the TC, TG, and LDL-C levels in the model group after the animals completed the atherogenic protocol were significantly higher than those in the control group (Table 1). Ultrasonic examinations showed that all 10 rabbits in the model group developed plaques. To improve the accuracy of our analysis, we identified the plaques with the largest diameters in each rabbit and performed two-dimensional ultrasound and color Doppler flow imaging to determine the locations of the plaques in question before performing CEUS (Figure 1).

Characterization of MBs

The Kurt counter results showed that the median diameter of MB_c was 2.26±0.01 μm, and the median diameter of MB_{IL-18} was 2.28±0.01 μm. The 2 MBs were uniformly dispersed. Fluorescence microscopy revealed that no fluorescence signal was present on the surface of MB_c; however, significant green fluorescence was present on the surface of MB_{IL-18}. Moreover, flow cytometry revealed that the IL-18 antibody was successfully conjugated to the MBs (Figure 2).

CEUS imaging of atherosclerotic plaques

CEUS imaging of MB_c and MB_{IL-18} revealed that both MBs were initially (approximately 2–4 s) located within the vessel lumen but then gradually dispersed to fill the base of the plaque and then the entire plaque. These findings indicate that MB_{IL-18} was as stable as MB_c. MB_{IL-18} had a greater signal intensity than MB_c (arbitrary intensity, 237.02± 6.75 *vs.* 201.73±17.85, *P*<0.05), indicating that MB_{IL-18} can enhance the echoes of the atherosclerotic plaques to a greater extent than MB_c. The TICs of MB_c and MB_{IL-18} showed that in the MB_{IL-18} images, the peak time was approximately 30 s, while in the MB_c images, the peak time was approximately 45 s, which indicated that plaques can be detected earlier by targeted MB. The TICs also showed that the peak intensity was higher and the contrast duration was longer in the targeted MB images than in the control MB images, suggesting that MB_{IL-18} was retained within the plaques and was thus able to facilitate the detection of atherosclerotic plaques (Figure 3).
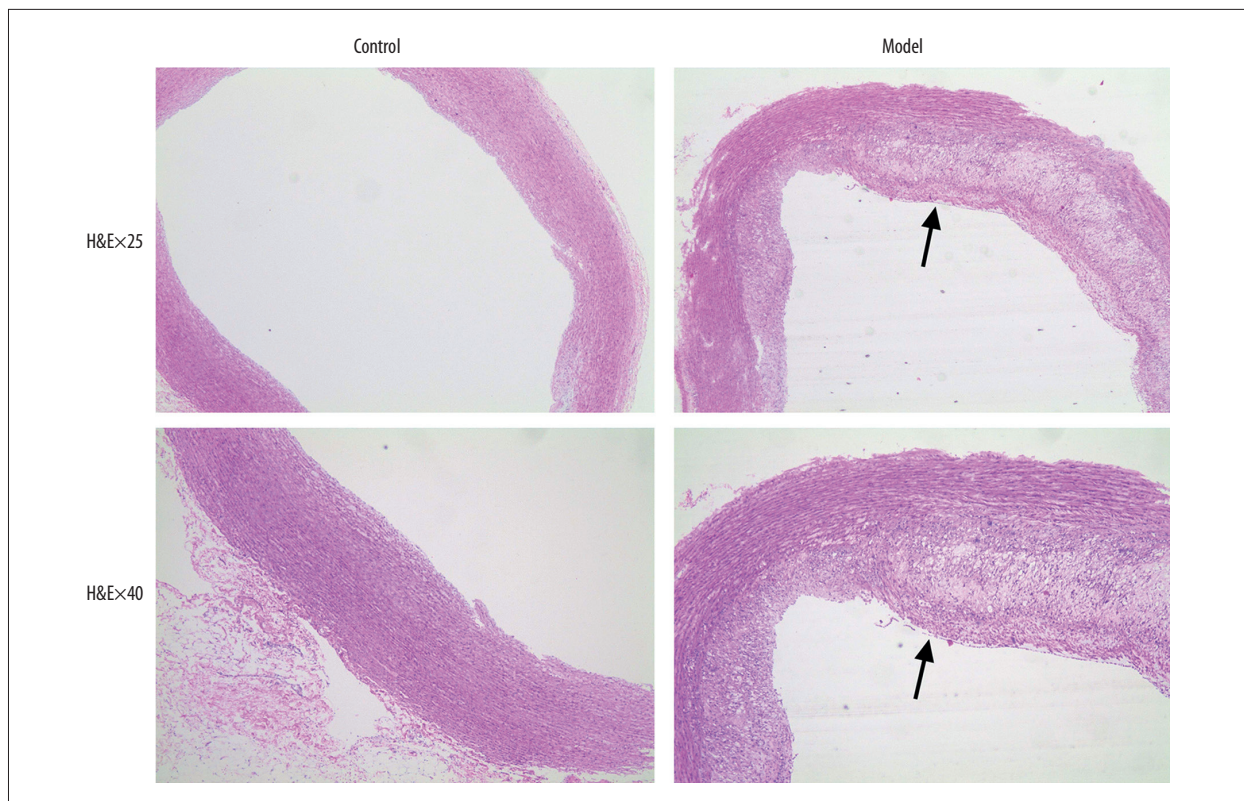
Figure 4. Representative histological images of rabbit aortas. In the normal group, the endothelial cells were arranged regularly, and there were no foam cells or lipid deposits in the intima. In the model group, the atherosclerotic lesion exhibited a thickened intima and many foam cells. Additionally, irregular apophysis was seen in the intima. The plaque is indicated by the arrowhead.

Histology and immunohistochemistry

All aortic atherosclerotic plaques detected by ultrasound were conclusively identified by histological examination. In the normal group, the endothelial cells were arranged regularly, and there were no foam cells or lipid deposits in the intima. In the model group, the atherosclerotic lesions had a thickened intima and many foam cells. Additionally, irregular apophysis was seen in the intima (Figure 4). Accordingly, the expression of CD34, which was used as a marker of plaque neovascularization, was significantly increased in the plaques. Immunohistochemistry also showed that IL-18 protein was mainly located in the inner parts and base of the atherosclerotic plaques, which was consistent with the enrichment of MB_{IL-18} during CEUS imaging (Figure 5).

IL-18 protein expression and its correlations with CEUS imaging

Rabbit arteries with and without atherosclerotic plaques (model and control groups, respectively) were used for protein expression analysis, and the results showed that the plaque regions of the model group had significantly higher IL-18 expression levels than the corresponding healthy regions of the control group (Figure 6). Correlation analysis showed that the contrast intensity of MB_{IL-18} was correlated with IL-18 expression ($r=0.903$, $P<0.05$), but the contrast intensity of MB_c was not correlated with IL-18 expression ($r=0.540$, $P>0.05$).

Discussion

Ultrasound molecular imaging of vulnerable plaques has attracted strong interest in the field of atherosclerotic plaque detection [10–12], and identifying molecular markers is a prerequisite for the accurate assessment of vulnerable plaques [16]. In the present study, we explored the specificity of IL-18 expression in atherosclerotic plaques and tested the ability of IL-18-targeted MBs to facilitate the identification of vulnerable plaques by ultrasound. To the best of our knowledge, this is the first to study the use of ultrasound to visualize the attachment of IL-18-targeted MBs to atherosclerotic plaques *in vivo*, and our findings suggest that such MBs may be a noninvasive and inexpensive tool with which to identify plaques with neovascularization.
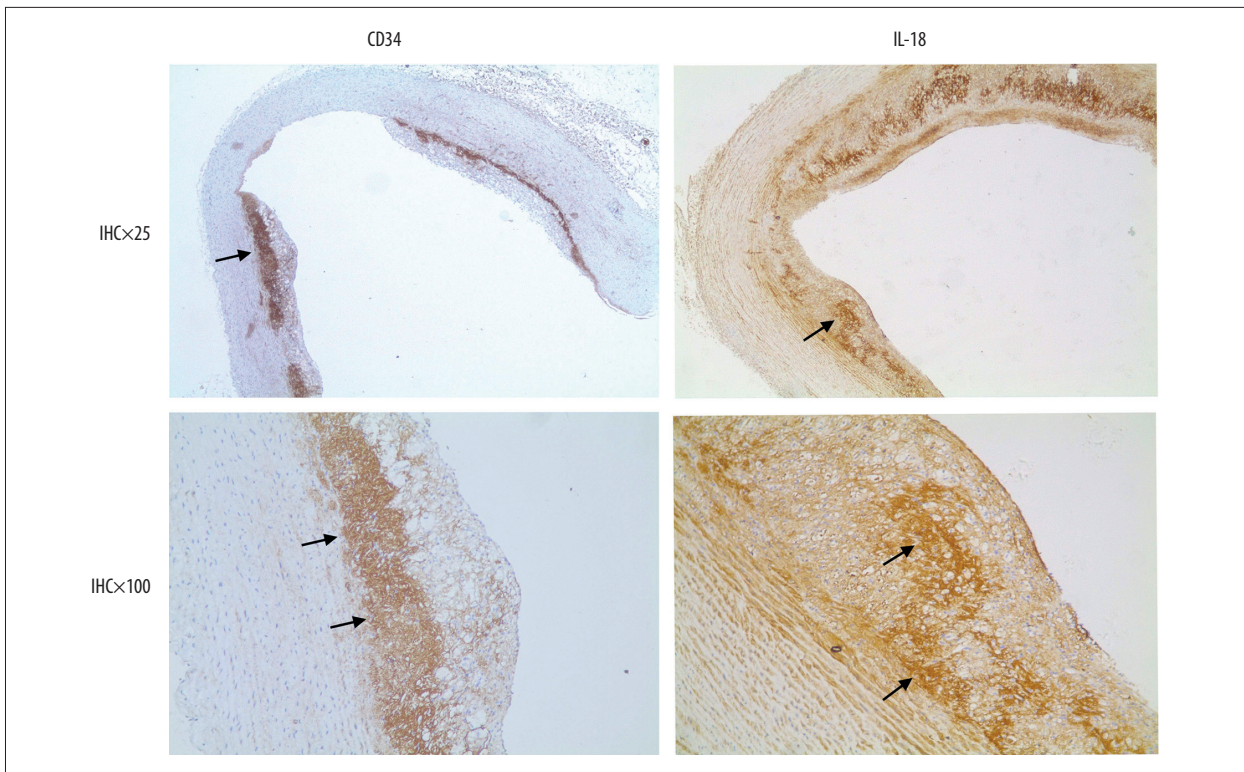
Figure 5. Immunohistochemical analysis of CD34 and IL-18 expression in atherosclerotic plaques in the rabbit aorta. Brown-stained areas indicated positive CD34 expression, which is denoted by the arrowheads. Immunohistochemistry also showed that IL-18 protein was mainly expressed in the inner parts and base of the atherosclerotic plaques.
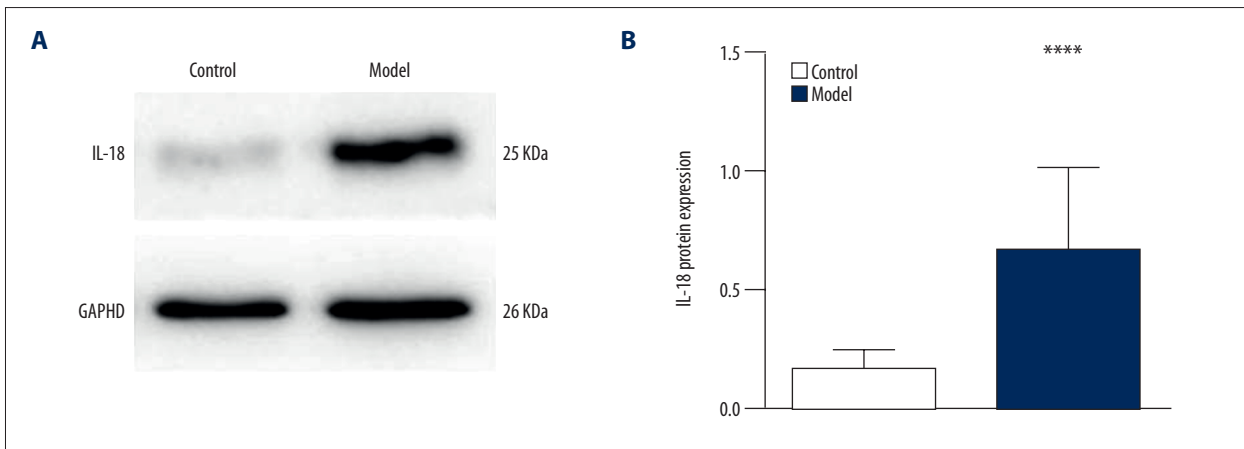

Figure 6. Quantification of IL-18 expression in plaques. (**A**) Significantly increased IL-18 expression was observed in the plaque regions. (**B**) Quantification of the data in (**A**). **** $P<0.0001$ versus the control group.

Several targeted MBs have been constructed with clinically suitable ligands and conjugation techniques [17,18]. Several studies have shown that biotin-streptavidin conjugation is an ideal method for conjugating specific antibodies to the surface of MBs. This method has been successfully used to develop antibody-conjugated MBs [11,15,19]. In the present study, a biotin-IL-18 antibody was conjugated to MBs via biotin-streptavidin conjugation, and the size, distribution, and macrostructural properties of the resulting MB_{IL-18} were stable. Immunofluorescence staining showed that only MB_{IL-18} emitted significant green fluorescence signals, and flow cytometry revealed that approximately 99.8% of the MBs were successfully conjugated to the IL-18 antibody. Both of these results indicate that the IL-18 antibody was successfully coupled to the surface of the MBs.

Atherosclerotic plaque rupture is considered a major cause of severe cardiovascular events, such as myocardial infarction and acute coronary syndrome [20]. Inflammatory factors, especially IL-18 (sometimes referred to as IFN-γ-inducing factor), and neovascularization-related inflammation participate in the process of plaque rupture [21]. Here, we determined that increased IL-18 expression is a marker of vulnerable plaques. IL-18, a novel cytokine, is secreted mainly by monocytes and macrophages. IL-18 expression reflects proinflammatory activity and can trigger specific immune reactions [22]. Specifically, IL-18 induces T cells and natural killer (NK) cells to produce IFN-γ and promotes the differentiation of T cells into Th1 cells to enhance the cell-mediated immune response. In addition, IL-18 induces the expression of IL-8, TNF-α, and adhesion molecules, which promote atherosclerotic plaque rupture [23].

CD34 was previously used to identify neovessels and was characterized as a marker of atherosclerosis [24]. In the present study, we observed that atherosclerotic plaques are rich with microvessels. Given that IL-18 participates in the process of plaque rupture, we used IL-18-targeted MBs to accurately identify atherosclerotic plaques, especially plaques that are vulnerable to rupture. We observed a significantly greater signal and earlier peak time in plaques injected with MB_{IL-18} than in plaques injected with MB_c. Additionally, we found that the MB_{IL-18} signal in the indicated plaques was sustained, which may be attributed to the adhesion of targeted MBs to the sites of inflammation-associated neovascularization inside plaques [25].

To elucidate the mechanism underlying the significant enrichment of IL-18-targeted MBs in atherosclerotic plaques, we analyzed IL-18 expression in plaque samples and the correlations between IL-18 expression and CEUS imaging. The result showed that IL-18 protein was mainly expressed in the inner parts and base of the atherosclerotic plaques and that higher IL-18 expression corresponded to more intense MB_{IL-18} contrast enhancement. Thus, the significant enrichment of IL-18-targeted MBs in plaques is dependent an increase in IL-18 expression in plaques.

A limitation of the present study was that we assessed only the largest plaques by two-dimensional ultrasound and CEUS. Additionally, we did not perform longitudinal studies to evaluate the differences in CEUS imaging of MB_{IL-18} between stable and vulnerable plaques.

Conclusions

In this study, we evaluated the behavior of MBs conjugated to the IL-18 antibody in a rabbit atherosclerotic plaque model. IL-18, which is also known as IFN-γ-inducing factor and participates in the process of plaque rupture, may be a marker of plaque neovascularization. IL-18-targeted MBs were found to exhibit higher contrast intensity and longer contrast durations in atherosclerotic plaques than naked MBs. Therefore, IL-18-targeted MBs may be an innovative method of detecting atherosclerotic plaques.

Conflict of interests

None.

References:

1. Steinl DC, Kaufmann BA: Ultrasound imaging for risk assessment in atherosclerosis. Int J Mol Sci, 2015; 16: 9749–69

2. Waxman S, Ishibashi F, Muller JE: Detection and treatment of vulnerable plaques and vulnerable patients: novel approaches to prevention of coronary events. Circulation, 2006; 114: 2390–411

3. Xia J, Yin A, Li Z et al: Quantitative analysis of lipid-rich necrotic core in carotid atherosclerotic plaques by *in vivo* magnetic resonance imaging and clinical outcomes. Med Sci Monit, 2017; 6: 2745–50

4. Macioch JE, Katsamakis CD, Robin J et al: Effect of contrast enhancement on measurement of carotid artery intimal medial thickness. Vasc Med, 2004; 9: 7–12

5. Rafailidis V, Pitoulias G, Kouskouras K, Rafailidis D: Contrast-enhanced ultrasonography of the carotids. Ultrasonography, 2015; 34: 312–23

6. You XD, Huang PT, Zhang C et al: Relationship between enhanced intensity of contrast enhanced ultrasound and microvessel density of aortic atherosclerotic plaque in rabbit model. PLoS One, 2014; 9: e92445

7. Zhou Y, Li Y, Bai Y et al: An assessment of the vulnerability of carotid plaques: A comparative study between intraplaque neovascularization and plaque echogenicity. BMC Med Imaging, 2013; 13: 13

8. Schinkel AF, Kaspar M, Staub D: Contrast-enhanced ultrasound: Clinical applications in patients with atherosclerosis. Int J Cardiovasc Imaging, 2016; 32: 35–48

9. Jiang ZZ, Xia GY, Zhang Y et al: Attenuation of hepatic fibrosis through ultrasound-microbubble-mediated HGF gene transfer in rats. Clin Imaging, 2013, 37: 104–10

10. Liu Y, Davidson BP, Yue Q et al: Molecular imaging of inflammation and platelet adhesion in advanced atherosclerosis effects of antioxidant therapy with NADPH oxidase inhibition. Circ Cardiovasc Imaging, 2013; 6: 74–82

11. Zhang YJ, Bai DN, Du JX et al: Ultrasound-guided imaging of junctional adhesion molecule-A-targeted microbubbles identifies vulnerable plaque in rabbits. Biomaterials, 2016; 94: 20–30

12. Metzger K, Vogel S, Chatterjee M et al: High-frequency ultrasound-guided disruption of glycoprotein VI-targeted microbubbles targets atheroprogression in mice. Biomaterials, 2015; 36: 80–89

13. Guo S, Shen S, Wang J et al: Detection of high-risk atherosclerotic plaques with ultrasound molecular imaging of glycoprotein IIb/IIIa receptor on activated platelets. Theranostics, 2015; 5: 418–30

14. Bouki KP, Katsafados MG, Chatzopoulos DN et al: Inflammatory markers and plaque morphology: An optical coherence tomography study. Int J Cardiol, 2012; 154: 287–92

15. Lai P, Du JR, Zhang MX et al: Aqueous extract of *Gleditsia sinensis* Lam. fruits improves serum and liver lipid profiles and attenuates atherosclerosis in rabbits fed a high-fat diet. J Ethnopharmacol, 2011; 137: 1061–66

16. Wei S, Fu N, Sun Y et al: Targeted contrast-enhanced ultrasound imaging of angiogenesis in an orthotopic mouse tumor model of renal carcinoma. Ultrasound Med Biol, 2014; 40: 1250–59

17. Barua A, Yellapa A, Bahr JM et al: Interleukin 16- (IL-16-) targeted ultrasound imaging agent improves detection of ovarian tumors in laying hens, a preclinical model of spontaneous ovarian cancer. BioMed Res Int, 2015; 2015: 567459

18. Anderson CR, Hu X, Zhang H et al: Ultrasound molecular imaging of tumor angiogenesis with an integrin targeted microbubble contrast agent. Invest Radiol, 2011; 46: 215–24

19. Yan F, Xu X, Chen Y et al: A lipopeptide-based alphavbeta(3) integrin-targeted ultrasound contrast agent for molecular imaging of tumor angiogenesis. Ultrasound Med Biol, 2015; 41: 2765–73

20. Zhang C, Huang P, Zhang Y et al: Anti-tumor efficacy of ultrasonic cavitation is potentiated by concurrent delivery of anti-angiogenic drug in colon cancer. Cancer Lett, 2014; 347: 105–13

21. Naghavi M, Libby P, Falk E et al: From vulnerable plaque to vulnerable patient: A call for new definitions and risk assessment strategies: Part I. Circulation, 2003; 108: 1664–72

22. Mathiesen EB, Bonaa KH, Joakimsen O: Echolucent plaques are associated with high risk of ischemic cerebrovascular events in carotid stenosis: The Tromso Study. Circulation, 2001; 103: 2171–75

23. Pigarevskii PV, Maltseva SV, Snegova VA et al: Role of interleukin-18 in destabilization of the atherosclerotic plaque in humans. Bull Exp Biol Med, 2014; 157: 821–24

24. Ragino YI, Chernyavski AM, Polonskaya YV et al: Activity of the inflammatory process in different types of unstable atherosclerotic plaques. Bull Exp Biol Med, 2012; 153: 186–89

25. Lu Y, Wei J, Shao Q et al: Assessment of atherosclerotic plaques in the rabbit abdominal aorta with interleukin-8 monoclonal antibody-targeted ultrasound microbubbles. Mol Biol Rep, 2013; 40: 3083–92